MCB
Journals.ASM.org

TRIM24 Is a p53-Induced E3-Ubiquitin Ligase That Undergoes ATM-Mediated Phosphorylation and Autodegradation during DNA Damage

Abhinav K. Jain, Kendra Allton, Aundrietta D. Duncan, Michelle C. Barton

Program in Genes and Development, University of Texas Graduate School of Biomedical Sciences at Houston, and Department of Biochemistry and Molecular Biology, Center for Stem Cell and Developmental Biology, University of Texas M. D. Anderson Cancer Center, Houston, Texas, USA

Tumor suppressor p53 protects cells from genomic insults and is a target of mutation in more than 50% of human cancers. Stress-mediated modification and increased stability of p53 promote p53 interaction with chromatin, which results in transcription of target genes that are critical for the maintenance of genomic integrity. We recently discovered that TRIM24, an E3-ubiquitin ligase, ubiquitinates and promotes proteasome-mediated degradation of p53. Here, we show that TRIM24 is destabilized by ATM-mediated phosphorylation of TRIM24S768 in response to DNA damage, which disrupts TRIM24-p53 interactions and promotes the degradation of TRIM24. Transcription of *TRIM24* is directly induced by damage-activated p53, which binds p53 response elements and activates expression of *TRIM24*. Newly synthesized TRIM24 interacts with phosphorylated p53 to target it for degradation and termination of the DNA damage response. These studies indicate that TRIM24, like MDM2, controls p53 levels in an autoregulatory feedback loop. However, unlike MDM2, TRIM24 also targets activated p53 to terminate p53-regulated response to DNA damage.

Tumor suppressor p53 maintains the genomic integrity of a cell in response to a variety of cellular stresses, including DNA damage, oncogenic stress, telomere dysfunction, and hypoxia (1–3). When exposed to stress stimuli, p53 acts as a central relay to determine how the cells respond, whether by apoptosis, cell cycle arrest, senescence, DNA repair, shifts in cell metabolism, or autophagy (4). Multiple signaling pathways converge on p53 to control its protein stability and activities, primarily by posttranslational modifications (PTMs) of p53 at specific amino acid residues (5–7). One of the major pathways that negatively regulate p53 protein stability is the ubiquitin-proteasome system, which adds polymerized chains of ubiquitin to p53 to target it for degradation (8, 9). The importance of this mechanism for cellular homeostasis is illustrated by p53-dependent embryonic lethality with germ line deletion of murine *Mdm2* (10), the first identified E3-ubiquitin ligase for p53 (11–13). However, a striking observation is that p53 degradation occurs even in Mdm2-deficient mouse tissues during cellular recovery after DNA damage (14). In addition, a recent report suggests that the p53-MDM2 feedback loop is dispensable for p53 stability after DNA damage *in vivo* (15). This suggested that a negative-feedback loop, which controls p53 protein levels, remains operable even in the absence of Mdm2. A collection of more than 15 E3-ubiquitin ligases that directly regulate p53 stability, including Pirh2, COP1, ARF-BP1 and others, are now known (16–18). These ligases stimulate p53 ubiquitination and degradation by directly modifying lysine residues, but their specific or redundant roles in regulation of p53 and how they themselves are regulated remain largely unknown.

We found that TRIM24 was an E3-ubiquitin ligase that negatively regulates p53 by directly targeting p53 for ubiquitination via a conserved RING domain (19). TRIM24 belongs to a large family of TRIM/RBCC proteins that are characterized by the presence of a conserved amino-terminal tripartite motif: a RING domain, B-box zinc fingers, and a coiled-coil region, along with variable carboxy-terminal domains (20, 21). TRIM24 was originally identified as transcriptional intermediary factor 1α (TIF-1α), a ligand-dependent corepressor of retinoic acid receptor alpha (22). TRIM24 is able to read dual histone marks by means of its tandem PHD (plant homeo domain) and bromodomain regions and facilitates the recruitment of estrogen receptor (ER) to chromatin regulatory sites. It is aberrantly expressed in human breast cancers and correlates with poor survival (23). Thus, aberrant expression of TRIM24 may promote tumor development and progression by coactivating estrogen receptor functions and/or by negatively regulating p53 activity. Interestingly, levels of TRIM24 must be carefully balanced, and its functions must be regulated in a tissue-specific manner, as genetic deletion of Trim24 ($Trim24^{-/-}$) results in retinoid-dependent liver tumorigenesis in mice (24). The mechanisms by which TRIM24 is regulated remain unknown, as is the identity of any signal transduction pathway that regulates the TRIM24-p53 axis after DNA damage. A better understanding of the signaling events that regulate TRIM24 is critical to uncover the basis for tissue-specific readouts of TRIM24 expression and realize the therapeutic potential of targeting TRIM24 in specific cancers.

Here, we describe an autoregulatory mechanism that dictates the response of the TRIM24-p53 axis during DNA damage and does so independently of MDM2. In response to DNA damage signals, p53-dependent transcriptional response is amplified by virtue of posttranslational modifications of p53 followed by its stabilization. During the process of p53 activation, DNA damage-induced signals likewise regulate TRIM24 but in the opposite direction to destabilize TRIM24. DNA damage induces enzymatic

Received 16 December 2012 **Returned for modification** 28 January 2013
Accepted 1 May 2014
Published ahead of print 12 May 2014
Address correspondence to Michelle C. Barton, mbarton@mdanderson.org.
Supplemental material for this article may be found at http://dx.doi.org/10.1128/MCB.01705-12.

doi:10.1128/MCB.01705-12

activity of ATM kinase and direct phosphorylation of serine 768 (S768) on TRIM24, rendering it unstable and a target for self-destruction by ubiquitination. With increased stability of p53 during DNA damage response, expression of *TRIM24* is induced in a p53-dependent manner by virtue of p53 binding to response elements (p53REs) in the distal promoter region of the *TRIM24* gene. As DNA damage response wanes, p53-induced *TRIM24* transcription and translation return TRIM24 to normal levels. Newly synthesized TRIM24 then targets phosphorylated p53 for degradation, bringing p53 levels back to their normal threshold in cells during homeostasis. Therefore, TRIM24 acts in an autoregulatory feedback loop that controls p53 levels prior to and at the termination of the stress response.

MATERIALS AND METHODS

Cell lines, treatments, and plasmids. MCF7, U2OS, and HEK293T cells were obtained from ATCC and cultured under suggested conditions in Dulbecco modified Eagle medium (DMEM) containing 10% fetal bovine serum (FBS), 1% L-glutamine, and 1% ampicillin-streptomycin. Val5 mouse embryonic fibroblasts (MEFs) were cultured as described before (25). MCF7 cells stably expressing nontarget or TRIM24 short hairpin RNA (shRNA) (shControl or shTRIM24, respectively) were described previously (23) and were cultured in complete DMEM containing 2.5 μg/ml puromycin. Mouse embryonic stem (ES) cells stably depleted of Trim24 were cultured as described previously (19). Wild-type (WT) (GM03490) and ATM-null ($ATM^{-/-}$) (GM02052) fibroblasts were obtained from Coriell Cell Repositories and cultured under suggested conditions in complete DMEM. WT and p53-null ($p53^{-/-}$) mouse embryonic stem (mES) cells were cultured in complete DMEM containing 20% FBS, β-mercaptoethanol, and 10 ng/ml leukemia inhibitory factor on gelatin-coated plates. The cells were treated with the following DNA-damaging agents: adriamycin (Adr) at either low (100- or 250-ng/ml) or high (500-ng/ml) doses and actinomycin D (10 ng/ml) for the times indicated in the figures; for ionizing radiation (IR), cells were exposed to 5 or 10 Gy of irradiation and then allowed to rest for the indicated times before harvesting. In some cases, cells were treated with MG132 (20 μM) for a total of 8 h. Nutlin-3 was obtained from Sigma, and MCF7 cells were treated for 24 h. Flag-tagged human full-length and N-terminal RING domain-truncated TRIM24, histidine-tagged ubiquitin (His-Ub), and pCMV-MDM2 (CMV stands for cytomegalovirus) were described previously (19). His-Xpress-Ub and pCMV-His-Ub plasmids were gifts from Sharon Dent's laboratory (University of Texas M. D. Anderson Cancer Center). ATM kinase site mutants of Flag-tagged TRIM24 (Flag-TRIM24) were made using the QuikChange XL site-directed mutagenesis kit (Stratagene) using the following primers: TRIM24-S217A Forward (5′-GGCAGTTGGTGTCACCGCCCAGCGACCAGTGTTTTGTCC) and Reverse (5′-GGACAAAACACTGGTCGCTGGGCGGTGACACCAACT GCC) primers, TRIM24-S768A Forward (5′-CCTGCTCTTAAATAGCG CCCAGAGCTCTACTTCTGAGG) and Reverse (5′-CCTCAGAAGTA GAGCTCTGGGCGCTATTTAAGAGCAGG) primers, and TRIM24-S768D Forward (5′-ACCTCCCTGCTCTTAAATAGCGATCAGAGCTC TACTTCTGAG) and Reverse (5′-CTCAGAAGTAGAGCTCTGATCG CTATTTAAGAGCAGGGAGGT) primers. All the plasmids were confirmed by sequencing before use.

Plasmid DNA and siRNA transfection. Cells were transfected with plasmids encoding human MDM2, Flag-TRIM24, Flag-TRIM24ΔRING, His-Ub, or phosphomutants of Flag-TRIM24 using Effectene (Qiagen) and following the manufacturer's recommendations. Oligonucleotide pools of small interfering RNA (siRNA) targeting human *TRIM24*, *TP53*, *MDM2*, and nontarget (control) were purchased from Dharmacon, and 75 nM was transfected into cells using Lipofectamine 2000 (Invitrogen) transfection reagent according to the manufacturer's protocol. Twenty-four hours after DNA transfection and 48 h after siRNA transfection, MCF7 cells were treated with DNA-damaging agents or MG132, as described earlier. The cells were then harvested and processed for protein or gene expression analyses.

RNA isolation and real-time PCR analysis. RNA was isolated using TRIzol reagent (Invitrogen) per the manufacturer's specifications. For RNA analysis, 500 ng total RNA was treated with DNase I, and cDNA was synthesized as previously described (19) and amplified with human gene-specific primers (see Table S1 in the supplemental material) with Power SYBR green PCR master mix (Applied Biosystems). The average threshold cycle (C_T) was determined for each gene and normalized to *Actin* mRNA level for internal normalization control. Fold mRNA levels were calculated and plotted.

Western blotting. Cells were lysed in radioimmunoprecipitation assay (RIPA) buffer (50 mM Tris [pH 8.0], 150 mM NaCl, 1% NP-40, 0.5% deoxycholic acid, 0.1% sodium dodecyl sulfate [SDS], and 1 mM phenylmethylsulfonyl fluoride [PMSF]) supplemented with protease inhibitor cocktail (Calbiochem) and phosphatase inhibitor cocktails I and II (Sigma). The protein concentration was estimated by the Bradford protein assay kit (Bio-Rad). Fifty micrograms of cell lysate was then separated using SDS-polyacrylamide gel electrophoresis (SDS-PAGE) and transferred to a nitrocellulose membrane. The membrane was blocked with 5% milk, and protein levels were analyzed by immunoblotting with anti-p53 (DO1; Santa Cruz), anti-Flag (Sigma), anti-TRIM24 (Novus Biologicals), MDM2 (Calbiochem), anti-ATM (Abcam), antibody against ATM with serine at position 1981 phosphorylated (anti-pSer1981ATM) (Millipore), antiubiquitin (Sigma), antibody against phosphorylated Chk2 (checkpoint kinase 2) (anti-pChk2) (Cell Signaling), and antiactin (GeneTex Biotechnology), followed by the corresponding horseradish peroxidase-tagged secondary antibody (GE Healthcare).

Subcellular fractionation. MCF7 and HEK293T cells were grown on 100-mm tissue culture plates and treated as described in the figure legends. At the end of treatment, the cells were washed twice with ice-cold phosphate-buffered saline (PBS), scraped off into PBS, and centrifuged at 500 rpm for 5 min. Biochemical fractionation of cells was done using the nuclear extraction kit (Active Motif, Inc.) according to the manufacturer's protocol. Briefly, the cell pellet was resuspended in 1× hypotonic buffer (cytoplasmic buffer) supplemented with complete protease inhibitor mixture (Calbiochem), incubated for 15 min at 4°C, vortexed in the presence of detergents, and centrifuged at 14,000 × *g* for 30 s. The supernatant (cytoplasmic fraction) was collected into a prechilled microcentrifuge tube. The nuclear pellet was washed twice with cytoplasmic buffer, followed by resuspension in nuclear lysis buffer supplemented with 1 mM dithiothreitol (DTT) and protease inhibitors. The suspension was incubated on a rocking platform at 4°C for 30 min, vortexed briefly, and centrifuged for 10 min at 14,000 × *g* at 4°C, and the supernatant (nuclear fraction) was collected. The protein concentration was determined using the protein assay reagent (Bio-Rad). Fifty micrograms of the cell fractions were resolved using 10% SDS-PAGE, analyzed by Western blotting, and probed with anti-TRIM24 and anti-p53 antibodies. To confirm the purity of subcellular fractionation, the extracts were immunoblotted with cytoplasm-specific anti-lactate dehydrogenase antibody (Chemicon) and nucleus-specific anti-PCNA antibody (Santa Cruz Biotechnology). Protein bands on immunoblots were quantitated using ImageJ software, normalized to actin, and plotted as fold changes in the level of protein in the nucleus.

Measurements of TRIM24 half-life. MCF7 cells were transfected with mock Flag vector, Flag-TRIM24, or phosphomutants of TRIM24 (Flag-TRIM24S217A, Flag-TRIM24S768A, or Flag-TRIM24S217/S768A double mutant) for 24 h and treated with the protein synthesis inhibitor cycloheximide at 30 μg/ml for different time points prior to analysis. To analyze the half-life of TRIM24 after adriamycin treatment, cells were pretreated with adriamycin for 4 h, followed by treatment with cycloheximide plus adriamycin simultaneously. Protein levels were quantified as described above and plotted as the percentage of remaining protein against time of cycloheximide treatment to calculate the half-life of p53. In a similar experiment, untransfected MCF7 cells were treated with cyclo-

heximide in the presence and absence of adriamycin and analyzed to detect the half-lives of endogenous TRIM24 and p53 proteins.

Coimmunoprecipitation analysis. MCF7 cells transfected with the indicated plasmids or treated with the DNA-damaging agents adriamycin or ionizing radiation, as indicated in the figures, were harvested and lysed in RIPA buffer. One milligram of cell lysates was used for immunoprecipitation with the primary antibody. The extract was incubated with 2.5 μg of antibody overnight at 4°C with shaking. Forty microliters of washed protein A bead suspension (GE Healthcare) was added and incubated for an additional 1 h at 4°C with shaking. Immunocomplexes were washed twice with RIPA buffer, boiled with 1× SDS sample dye, and resolved on 10% SDS-polyacrylamide gels, followed by immunoblotting with the corresponding antibodies.

***In vitro* phosphatase assay.** MCF7 cells treated with DNA-damaging agents, adriamycin (500 ng/ml), or exposed to IR (10 Gy), for 1 h were harvested and lysed in RIPA buffer without phosphatase inhibitors. Thirty-microgram amounts of lysates were incubated with 2 U of shrimp alkaline phosphatase (Roche) in phosphatase buffer (150 mM NaCl, 50 mM Tris [pH 8.5], 5 mM $MgCl_2$, and 1 mM DTT) for 45 min at 32°C, boiled with 1× SDS sample dye, and resolved on 4 to 12% Bis-Tris gradient gel (Invitrogen), followed by immunoblotting with TRIM24 antibody (Protein Technology). For analyzing TRIM24-p53 interaction after phosphatase treatment, MCF7 cells were transfected with Flag-TRIM24 plasmid and exposed to ionizing radiation (10 Gy) for 30 min or 2 h. The cells were harvested and lysed in RIPA buffer without phosphatase inhibitors. One-milligram amounts of lysates were incubated with 2 U of calf intestinal phosphatase (CIP) in phosphatase buffer for 1 h at 32°C and subjected to immunoprecipitation with Flag antibody, followed by immunoblotting with Flag and p53 antibodies.

Endogenous p53 ubiquitination assay. MCF7 cells were transfected with plasmids as indicated in the figures. Cells were treated with the proteasome inhibitor MG132 (Calbiochem) for 6 h prior to lysis in RIPA buffer supplemented with 10 mM iodoacetamide (GE Healthcare) and protease inhibitors. Endogenous p53 was immunoprecipitated from 1 mg protein lysate using p53 (DO1) antibody and immunoblotted with antiubiquitin antibody (Sigma). The blot was reprobed with p53 to confirm the equal p53 pulldown.

TRIM24 ubiquitination assay. MCF7 cells were transfected with plasmids expressing Flag-TRIM24 and His-ubiquitin, as indicated in the figures. Cells were treated with the proteasome inhibitor MG132 (Calbiochem) for 6 h prior to lysis in binding buffer (20 mM sodium phosphate, 500 mM NaCl, 20 mM imidazole [pH 7.3]) supplemented with 10 mM iodoacetamide (GE Healthcare) and protease inhibitors. Ubiquitin-tagged proteins were purified on an Ni column (GE Healthcare) following the manufacturer's protocol and eluted in buffer containing 250 mM imidazole. Detection of TRIM24 ubiquitination under denaturing conditions was performed as described previously (26). Briefly, MCF7 cells were transfected and lysed in lysis buffer (6 M guanidinium hydrochloride [G-HCl], 0.1 M phosphate buffer, 5 mM imidazole [pH 8]) supplemented with protease inhibitors and NEM (*N*-ethylmaleimide). The lysates were passed through the Ni column and eluted in buffer (50 mM phosphate buffer, 100 mM KCl, 20% glycerol, 0.2% NP-40, and 200 mM imidazole [pH 8]). Eluted fractions were resolved on 4 to 12% Bis-Tris gradient gel followed by immunoblotting with Flag antibody to detect ubiquitinated Flag-TRIM24 proteins.

TRIM24 phosphorylation analysis. MCF7 cells were transfected with mock Flag vector, Flag-TRIM24, or phosphomutants of TRIM24 (Flag-TRIM24S217A, Flag-TRIM24S768A, or Flag-TRIM24S217/S768-A double mutant) for 24 h and exposed to IR for 30 min or 1 h in the absence or presence of MG132. The cells were then harvested and lysed in RIPA buffer. One milligram of cell lysates was used for immunoprecipitation with anti-pS/T-ATM substrate antibody (Cell Signaling) to detect ATM kinase phosphorylated substrates. The extracts were incubated with 2.5 μg of antibody overnight at 4°C with shaking. Forty microliters of washed protein A bead suspension (GE Healthcare) was added and incubated for an additional 1 h at 4°C with shaking. Immunocomplexes were washed twice with RIPA buffer, boiled with 1× SDS sample dye, and resolved on 10% SDS-polyacrylamide gels, followed by immunoblotting with Flag antibody.

p53 chromatin immunoprecipitation (ChIP) analysis. Cells cultured in the required conditions and treated with the DNA-damaging agent adriamycin for different time points were collected, washed in PBS, and cross-linked in 1% formaldehyde for 10 min at room temperature. After the cross-linking reaction was terminated by the addition of glycine, followed by washing in PBS, the cells were lysed using lysis buffer (5 mM HEPES [pH 8.0], 85 mM KCl, 0.5% NP-40) supplemented with protease inhibitor (Calbiochem). After removal of the cytoplasmic extract, the remaining cell pellet was lysed in nuclear lysis buffer (50 mM Tris-HCl [pH 7.5], 10 mM EDTA, 1% SDS) and protease inhibitor. The lysates were sonicated with glass beads (Sigma) 10 times for a 10-s pulse on ice to obtain DNA fragments with an average length less than 500 bp. After centrifugation, the supernatant was preabsorbed with 40 μl protein A beads (GE Healthcare) and IgG for 2 h and then incubated with 5 μg p53 antibody (Santa Cruz Biotechnology) or control IgG (Millipore) overnight at 4°C. The immune complex was collected on protein A beads and washed, and the bound DNA was eluted and reverse cross-linked overnight at 65°C. The DNA region of interest was detected by SYBR real-time quantitative PCR (qPCR) using primers encompassing p53 response elements (p53REs) on the respective gene (see Table S2 in the supplemental material).

RESULTS

TRIM24 ubiquitinates p53 independently of MDM2. TRIM24 is a multifunctional protein that possesses several protein domains, which dictate its functions as an E3-ubiquitin ligase (RING domain), histone code reader (PHD and bromodomain), coregulator of ER (LXXLL motif), and cointeracting partner of a variety of proteins (coiled-coil domain) (21, 23). Previously, we reported that the RING domain of TRIM24 mediates ubiquitination and negative regulation of p53 in both mouse and human embryonic stem cells (19, 27). To further understand regulation of the TRIM24-p53 axis in cancer cells, we analyzed the ubiquitination status of p53 when TRIM24 was exogenously expressed or depleted in human breast cancer-derived MCF7 cells, which harbor wild-type p53 (Fig. 1A and B). Exogenous expression of either TRIM24 or MDM2 induced ubiquitination of p53 (Fig. 1A), whereas siRNA-mediated, transient depletion of TRIM24 significantly decreased ubiquitination of p53, comparable to MDM2 (Fig. 1B). A closely related family member of TRIM24, TRIM28 (also known as KAP1), was previously shown to play a role in p53 inactivation by directly interacting with MDM2 and enhancing its E3-ubiquitin ligase activity toward p53 (28). Therefore, we asked whether TRIM24 interacts with MDM2 to ubiquitinate p53. Cointeraction analysis in MCF7 cells treated with DNA-damaging agents, such as adriamycin (Adr) or ionizing radiation (IR), showed no detectable interaction between TRIM24 and MDM2, although TRIM24 bound to known partner TRIM33 (Fig. 1C). A similar analysis of human osteosarcoma (U2OS) cells, which aberrantly overexpress MDM2, also revealed no interaction between TRIM24 and MDM2 (Fig. 1D). Taken together, these results indicate that TRIM24 ubiquitinates p53 independently of MDM2.

DNA damage induces degradation of TRIM24 in the nucleus. DNA damage signals stabilize and activate p53, in parallel with downregulation of negative regulators of p53, such as MDM2 (29). We found that TRIM24 responds in a comparable manner: exposure of MCF7 cells to DNA-damaging agent actinomycin D or adriamycin over a time course reduced TRIM24 levels by

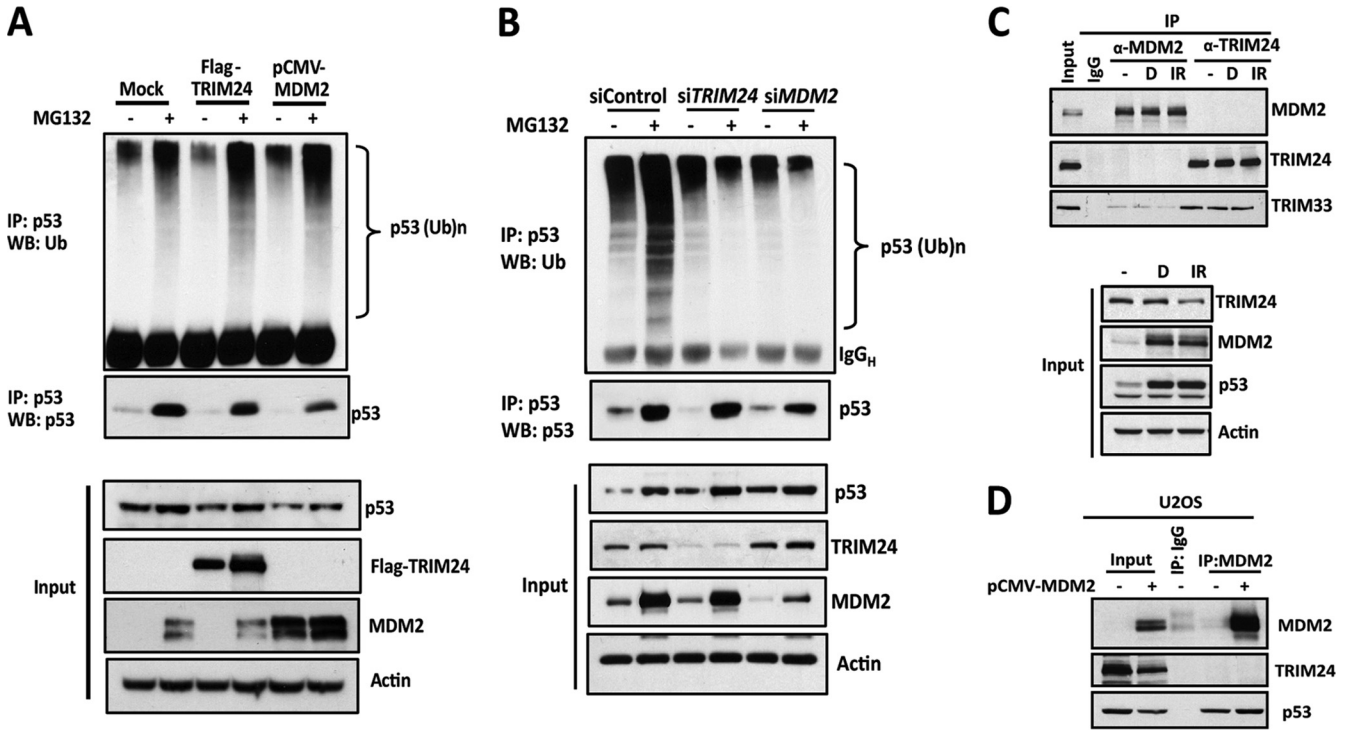

FIG 1 TRIM24 ubiquitinates p53 independently of MDM2. (A and B) Endogenous p53 ubiquitination. MCF7 cells transiently transfected with TRIM24 and MDM2 plasmids (A) or transiently transfected with control, *TRIM24*, and *MDM2* siRNA (B) were treated with MG132 (+) for 8 h. Total lysates were immunoprecipitated (IP) with p53 antibody and probed for ubiquitin (Ub). Inputs are shown in the bottom panels. WB, Western blotting. (C) TRIM24-MDM2 interaction. MCF7 cells were pretreated with MG132 for 4 h, followed by treatment with 250 ng/ml adriamycin (D) for 1 h or exposed to 10 Gy ionizing radiation (IR) and harvested after 1 h. Total cell lysates were immunoprecipitated with either TRIM24 or MDM2 antibody and immunoblotted. IgG served as a negative control for the immunoprecipitation reactions. (D) TRIM24-MDM2 interaction. Total lysates from U2OS cells transfected with pCMV-MDM2 were immunoprecipitated with MDM2 antibody and immunoblotted for MDM2, TRIM24, and p53.

~70% or ~80%, respectively, as p53 accumulated (~10-fold or ~18-fold, respectively) (Fig. 2A and B). Likewise, MDM2 levels decreased rapidly after adriamycin treatment, while p53 levels dramatically increased and remained relatively constant over the 24-h treatment period. When MCF7 cells were exposed to a brief pulse of DNA damage (4-h Adr treatment or IR exposure at time zero) and then allowed to recover, TRIM24 levels initially declined (60% remaining after Adr treatment and 20% remaining 2 h after IR treatment) and then increased at later time points during recovery (Fig. 2C). On the other hand, p53 levels were dramatically induced (up to 8-fold after Adr treatment and 16-fold after IR treatment) in an initial response to stress and returned to normal threshold levels at later time points (Fig. 2C). These results suggested that an inverse stoichiometry between TRIM24 and p53 is induced in response to DNA damage.

Previous studies show that p53 is regulated in part by nuclear-cytoplasmic shuttling and its activity as a transcription factor depends on its nuclear localization, which increases in response to stress (30) (Fig. 2D). Subcellular fractionation showed nuclear enrichment of TRIM24 in unstressed MCF7 cells, with levels decreasing over time of DNA damage, while p53 accumulated up to 10-fold in parallel with adriamycin treatment (Fig. 2D). We determined whether clearance of TRIM24 from the nucleus was the result of its nuclear export, rather than active degradation, in response to stress. In the presence of a nuclear export inhibitor, leptomycin B, TRIM24 accumulates in the nucleus (2-fold), suggesting that TRIM24 shuttles actively between cytosolic and nuclear compartments of unstressed cells (Fig. 2E). However, with adriamycin treatment, nuclear levels of TRIM24 were reduced even in the presence of leptomycin B, while p53 accumulated up to 16-fold within 1 h (Fig. 2E). These results indicate that TRIM24 is degraded in the nucleus during the active phase of the DNA damage response. DNA damage-mediated depletion of nuclear TRIM24 levels was also observed in HEK293T cells in the presence of either leptomycin B or the protein synthesis inhibitor cycloheximide (Fig. 2F and G; see Fig. S1A and B in the supplemental material). TRIM24 levels decrease, albeit at a lower rate, which may reflect a greatly attenuated p53 response in HEK293T cells. Furthermore, constitutive expression of adenoviral E1A/E1B proteins and simian virus 40 (SV40) large T antigen in HEK293T cells might also affect TRIM24 levels. Taken together, these results suggest that during the DNA damage response, while p53 is actively localized in the nucleus, there is a rapid turnover of TRIM24 that occurs independently of export from the nucleus.

TRIM24 undergoes ubiquitination-mediated degradation in response to DNA damage. DNA damage-mediated reduction in TRIM24 protein levels, as shown here, suggested that TRIM24 might undergo active degradation during stress response. We analyzed TRIM24 protein levels in cells treated with the proteasomal inhibitor MG132 to determine whether an ubiquitin-mediated pathway regulates TRIM24 protein levels. p53 levels were significantly (~13.5-fold) higher in MCF7 cells depleted of TRIM24 by shRNA (shTRIM24) compared to control, confirming that TRIM24 is a negative regulator of p53 (Fig. 3A). Interestingly,

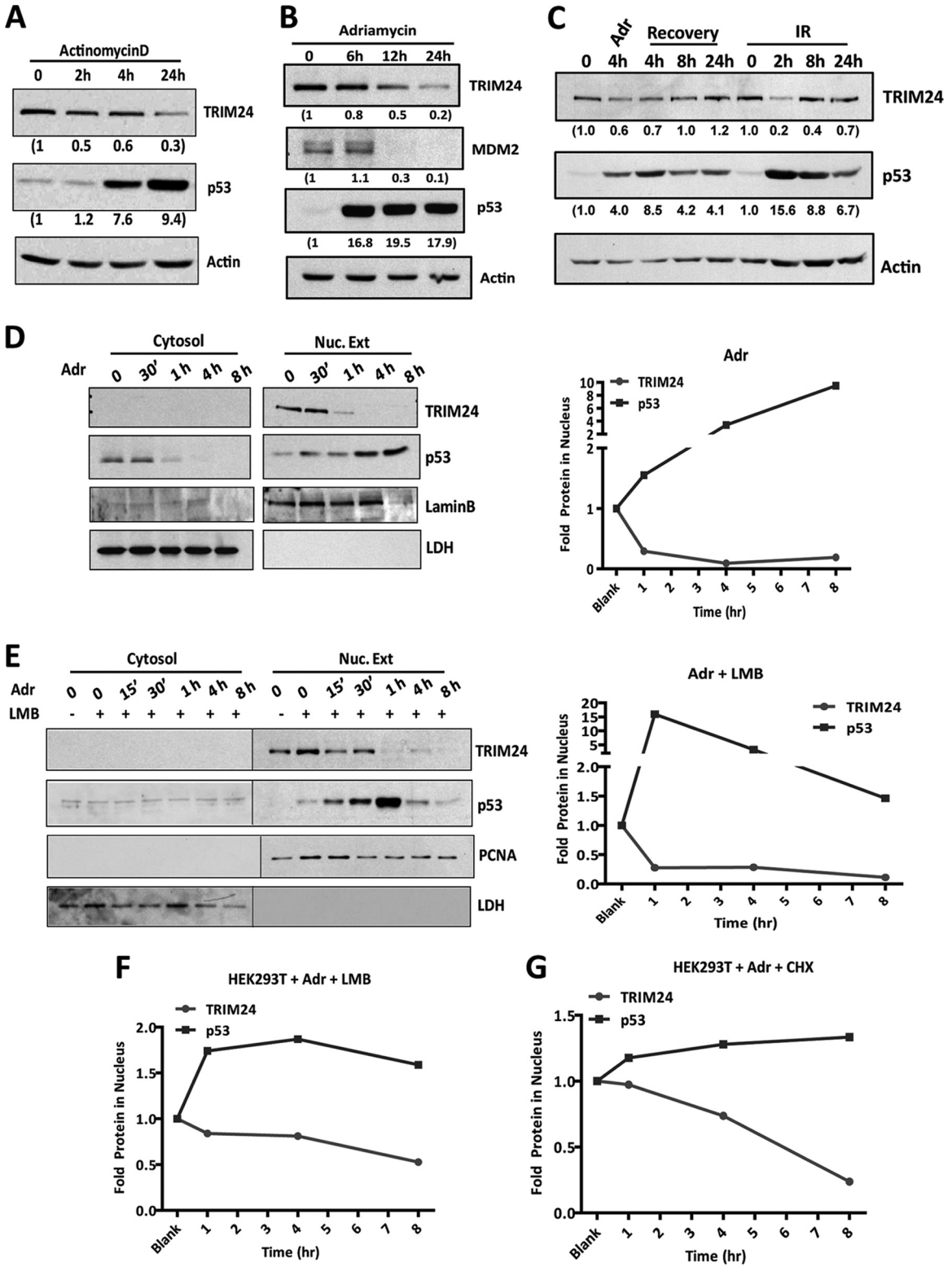

FIG 2 DNA damage induces degradation of TRIM24 in the nucleus. (A and B) MCF7 cells were treated with actinomycin D (10 ng/ml) (A) or high-dose adriamycin (Adr) (500 ng/ml) (B) for the indicated lengths of time, and total TRIM24, MDM2, and p53 were analyzed by Western blotting. (C) MCF7 cells were treated with adriamycin (250 ng/ml) for 4 h, followed by washing the medium and harvesting the cells at the indicated times, and total TRIM24, and p53 were analyzed by Western blotting. Blots were quantitated, and fold changes in total protein levels normalized to actin are shown in parentheses under the blots in panels A to C. (D and E) TRIM24 nuclear localization. Nuclear extracts (Nuc. Ext) prepared from MCF7 cells treated with adriamycin for different time points (0, 15 or 30 min, up to 8 h) in the absence (D) or presence (E) of the nuclear export inhibitor leptomycin B (LMB) were analyzed by Western blotting. Blots were quantitated, and fold changes in nuclear protein levels were plotted in the graphs to the right of the blots. (F and G) TRIM24 nuclear localization. Nuclear extracts prepared from HEK293T cells treated with Adr for different time points in the presence of LMB (F) or the protein synthesis inhibitor cycloheximide (CHX) (G) were analyzed by Western blotting. Blots were quantitated, and fold changes in nuclear protein levels were plotted.

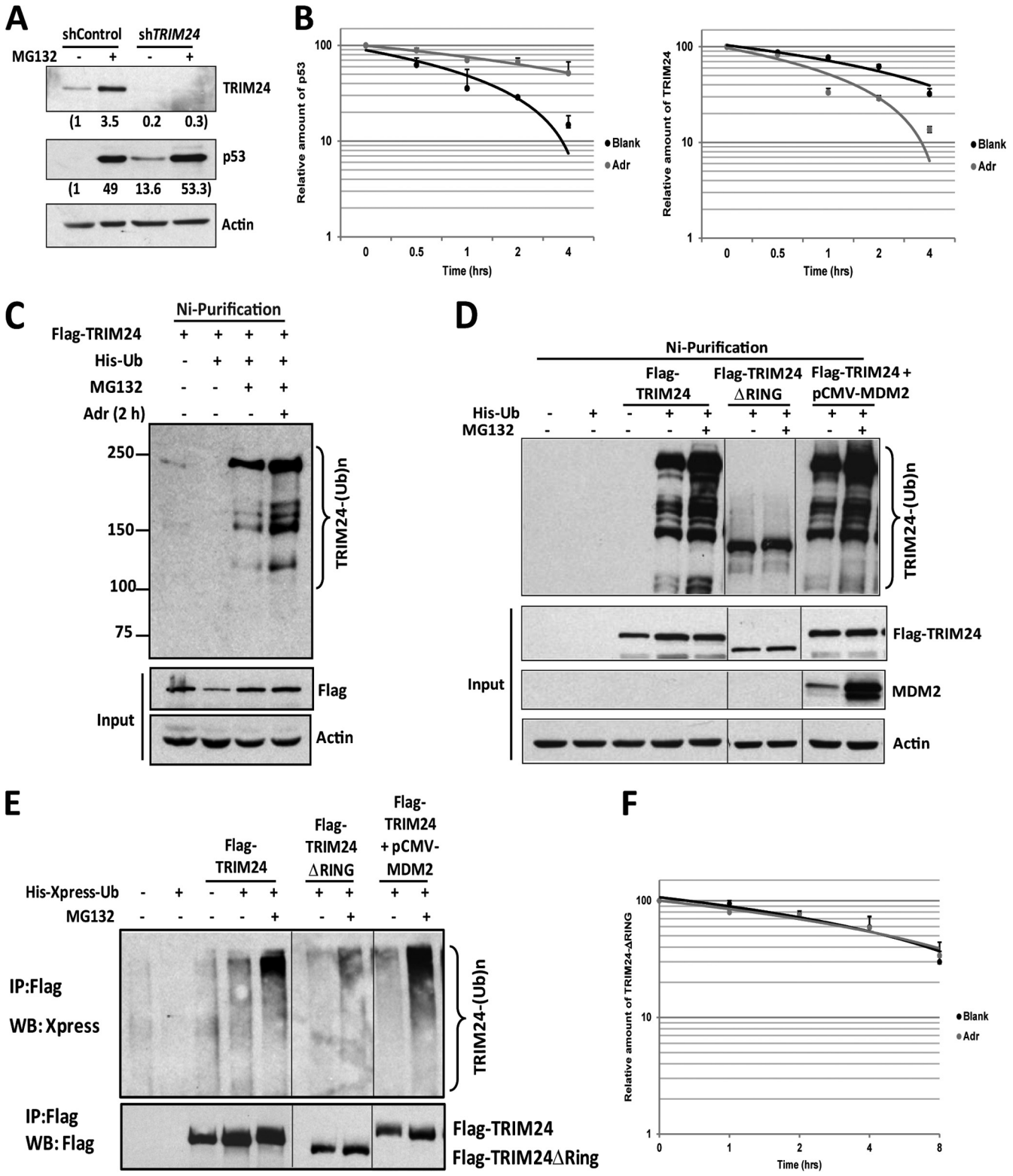

FIG 3 TRIM24 undergoes ubiquitination-mediated degradation in response to DNA damage. (A) MCF7 cells stably integrated with nontarget shRNA (shControl) or shRNA specific to *TRIM24* (sh*TRIM24*) were treated with MG132 for 8 h. Total p53 and TRIM24 were analyzed by Western blotting. (B) TRIM24 and p53 half-lives. MCF7 cells were treated with CHX for the indicated time points without (Blank) or with (Adr) DNA damage. p53 and TRIM24 protein levels were analyzed by immunoblotting, quantified by densitometry, and plotted against time to determine TRIM24 and p53 half-lives. (C) TRIM24 ubiquitination. MCF7 cells transiently transfected with Flag-TRIM24 and His-Ub plasmids were pretreated with MG132 for 6 h followed by treatment with Adr plus MG132. Total lysates were prepared under denaturing conditions. Equal amounts of lysates were purified on a Ni column and Western blotted with Flag antibody to detect ubiquitinated Flag-TRIM24. The positions of molecular size markers (in kilodaltons) are shown to the left of the gel. (D and E) TRIM24 autoubiquitination.

MG132 treatment resulted in stabilization of both TRIM24 and p53 in shControl cells and of only p53 in shTRIM24 cells (Fig. 3A). This suggested that TRIM24 undergoes proteasomal degradation in shControl cells, and multiple proteasome-dependent pathways impinge on p53 regulation in MCF7 cells. To quantify the specific effects of DNA damage versus protein synthesis in regulating stability, we analyzed the half-lives of endogenous p53 and TRIM24 proteins in the presence of cycloheximide, with and without DNA damage. p53 is a very short-lived, unstable protein with a half-life of ~30 min in MCF7 cells (31), but in response to DNA damage, p53 was stabilized with an extended half-life of ~3 h (Fig. 3B). In contrast, exposure to DNA damage resulted in a significant reduction in the half-life of TRIM24, from ~3 h to ~50 min (Fig. 3B; see Fig. S2A in the supplemental material), suggesting a rapid turnover of TRIM24 in response to damage. Similar results were observed in U2OS cells, which are also p53 responsive, when these cells were exposed to adriamycin (see Fig. S2B). Because TRIM24 is stabilized by MG132 treatment of shControl MCF7 cells (Fig. 3A), we reasoned that TRIM24 undergoes ubiquitin-mediated degradation.

Ubiquitination analysis of TRIM24 under denaturing conditions revealed that TRIM24 undergoes polyubiquitination, which is significantly increased in response to adriamycin treatment (Fig. 3C). TRIM24 possesses E3-ubiquitin ligase activity via its RING domain (19); therefore, we explored the possibility that TRIM24 ubiquitinates itself. In comparison to wild-type TRIM24, TRIM24 with a deletion of the RING domain (TRIM24-ΔRING) was greatly decreased in ubiquitination, as was apparent under both denaturing and nondenaturing conditions (Fig. 3D and E), which suggests that TRIM24 undergoes autoubiquitination. TRIM24-ΔRING is highly stable, and the half-life of TRIM24-ΔRING was unchanged with adriamycin treatment, suggesting that the RING domain mediates TRIM24 degradation (Fig. 3F; see Fig. S2C in the supplemental material). Neither exogenous expression nor RNA interference (RNAi)-mediated knockdown of MDM2 had an effect on TRIM24 ubiquitination, indicating that TRIM24 is not a substrate for MDM2's E3-ubiquitin ligase activity (Fig. 3D and E; see Fig. S2D). These observations indicate that TRIM24 is destabilized in response to DNA damage by proteasomal degradation as a result of autoubiquitination via its own RING domain.

Phosphorylation of S786 by ATM kinase induces TRIM24 degradation during DNA damage. Stress responses trigger signaling pathways that can dictate the stability or localization of proteins (32–34). TRIM24 E3-ubiquitin ligase functions were altered after treatment with DNA-damaging agents; this led us to ask whether there are specific signaling mechanisms that dictate the fate of TRIM24 under stress conditions. We used phosphorylation site prediction software (NetPhosK 1.0 server, Technical University of Denmark) to determine whether TRIM24 is a substrate for kinase-mediated phosphorylation and identified several sites in TRIM24 predicted to be targets of various kinases. Sites for ATM kinase were of particular interest; ATM kinase acts as a sentinel for DNA damage and phosphorylates key proteins, including p53, breast cancer-associated gene 1 (BRCA1), and checkpoint kinase 2 (Chk2) (35). p53 is stabilized in response to DNA damage (36, 37) via direct phosphorylation of p53Ser15 by ATM kinase (38). This results in increased interactions between p53 and transcriptional coactivator p300 and increased p53-regulated transcription (39). ATM also phosphorylates MDM2 and the related protein MDMX, to dampen their ability to negatively regulate p53 (32, 33, 40).

ATM kinase sites possess serine-glutamine (SQ) motifs surrounded by hydrophobic amino acids (41). TRIM24 contains six SQ motifs, with the second SQ motif, SQ2 (Ser217), and the fifth SQ motif, SQ5 (Ser768), being of primary interest, as they are highly conserved and fit the criteria for a consensus ATM motif (Fig. 4A; see Fig. S3A and B in the supplemental material). S768 phosphorylation of TRIM24 was also detected in a large-scale proteomic analysis of ATM kinase targets in response to DNA damage (42). Analysis of MCF7 cell lysates on a high-resolution gradient gel revealed a slower-migrating, higher-molecular-weight band of TRIM24 that increased when cells were treated with adriamycin or IR for 1 h and was abolished by treatment with shrimp alkaline phosphatase (SAP) *in vitro* (Fig. 4B), suggesting that DNA damage induced phosphorylation of TRIM24. We observed IR- and adriamycin-dependent activation of ATM kinase, revealed by increased ATM autophosphorylation (see Fig. S3C) (41, 43).

To confirm whether DNA damage-induced phosphorylation of TRIM24 is mediated by ATM kinase, lysates from Flag-TRIM24-transfected MCF7 cells exposed to IR in the absence or presence of MG132 were immunoprecipitated with antibody that specifically interacts with phosphorylated serine/threonine (S/T) residues targeted by ATM. Detection of Flag-TRIM24 in these protein complexes by immunoblotting with Flag antibody revealed bands specific for phosphorylated TRIM24 (Fig. 4C), which were abolished in lysates treated with SAP (see Fig. S3D in the supplemental material), confirming that TRIM24 is a likely substrate of ATM kinase, as is Chk2. The intensity of phosphorylated TRIM24 (phospho-TRIM24) decreased 2 h after IR exposure, a loss reversed by MG132 treatment, indicating that the phosphorylated form of TRIM24 is unstable and undergoes rapid degradation (Fig. 4C). We generated mutations of residues S217 and S768 of TRIM24 to encode alanine rather than serine (S271A and S768A), individually or as a double mutant (DM) (Fig. 4D). Phospho-S/T substrate analysis indicated that S768 is the preferred substrate of ATM kinase, although other residues might also be targeted, as ~25% of the S768 mutant protein remained phosphorylated (Fig. 4D). We then assessed the effect of ATM-mediated phosphorylation on TRIM24 half-life and observed that, in comparison to wild-type TRIM24 and TRIM24S217A, both TRIM24S768A and TRIM24DM were highly stable proteins. Adriamycin treatment did not significantly alter the stability of TRIM24S768A and TRIM24DM, as their half-lives after adriamycin treatment remained greater than 7 h (Fig. 4E; see Fig. S3E).

MCF7 cells transiently transfected with Flag-TRIM24, Flag-TRIM24ΔRING, or CMV-MDM2 plus His-Xpress-Ub were treated with MG132 for 8 h. (D) Total cell lysates prepared under denaturing conditions were subjected to Ni-purification followed by Western blotting with Flag antibody to detect ubiquitinated Flag-TRIM24. (E) In a similar experiment, total lysates were immunoprecipitated with Flag antibody, followed by immunoblotting with Xpress antibody to detect ubiquitinated Flag-TRIM24. (F) TRIM24ΔRING half-life. MCF7 cells transfected with Flag-TRIM24ΔRING were treated with CHX for different time points without (Blank) or with (Adr) DNA damage. TRIM24 protein levels were analyzed by immunoblotting with Flag antibody, quantified by densitometry, and plotted against time to determine TRIM24 half-lives.

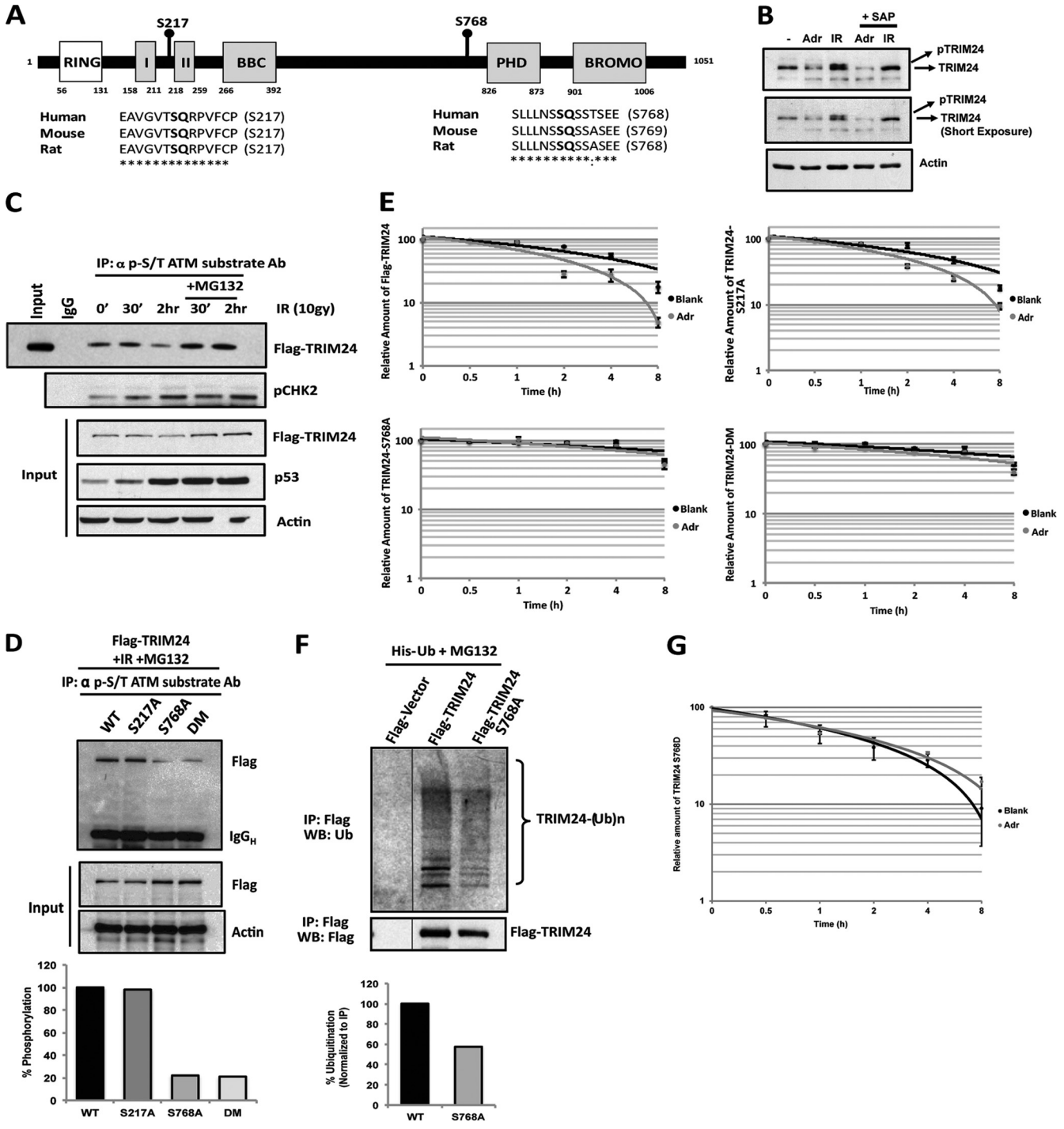

FIG 4 Phosphorylation at S768 by ATM kinase induces TRIM24 degradation during DNA damage. (A) ATM phosphorylation sites on TRIM24. Scheme representing two conserved ATM sites (S217 and S768) on TRIM24 proteins. I and II, B-box I and II; BBC, coiled-coil domain. (B) *In vitro* phosphatase assay. MCF7 cells were treated with Adr for 1 h or exposed to IR and allowed to rest for 1 h. Thirty micrograms of lysate was incubated with shrimp alkaline phosphatase (SAP) and analyzed by Western blotting. (C) TRIM24 phosphorylation. MCF7 cells transfected with Flag-TRIM24 were collected at 30 min and 2 h after IR with or without MG132 treatment. Total lysates were immunoprecipitated with anti-pS/T ATM substrate antibody and blotted with Flag to detect phosphorylated TRIM24. pChk2 was used as a control for ATM activation. Inputs are shown in bottom panels. (D) TRIM24 phosphorylation. MCF7 cells transfected with phosphosite mutants (S217A or S768A) of TRIM24 were treated and analyzed as described for panel C. The immunoprecipitated bands were quantitated, and the percent phosphorylation was plotted in the graph shown below the blots. (E) TRIM24 half-life. MCF7 cells transfected with wild-type or phosphomutants of Flag-TRIM24 were treated with CHX for different time points without (Blank) or with (Adr) DNA damage. TRIM24 protein levels were analyzed by immunoblotting with Flag antibody, quantified by densitometry, and plotted against time to determine TRIM24 half-lives. (F) TRIM24 ubiquitination. MCF7 cells transiently transfected with Flag-TRIM24 or Flag-TRIM24S768A plus His-Ub were treated with MG132. Total cell lysates were subjected to Flag immunoprecipitation followed by Western blotting with ubiquitin antibody to detect ubiquitinated Flag-TRIM24. The total Flag-TRIM24 immunoprecipitated is shown in the bottom blot. (G) TRIM24-S768D half-life. MCF7 cells were transfected with phosphomimic mutant Flag-TRIM24-S768D, and its half-life was assessed as described for panel E.

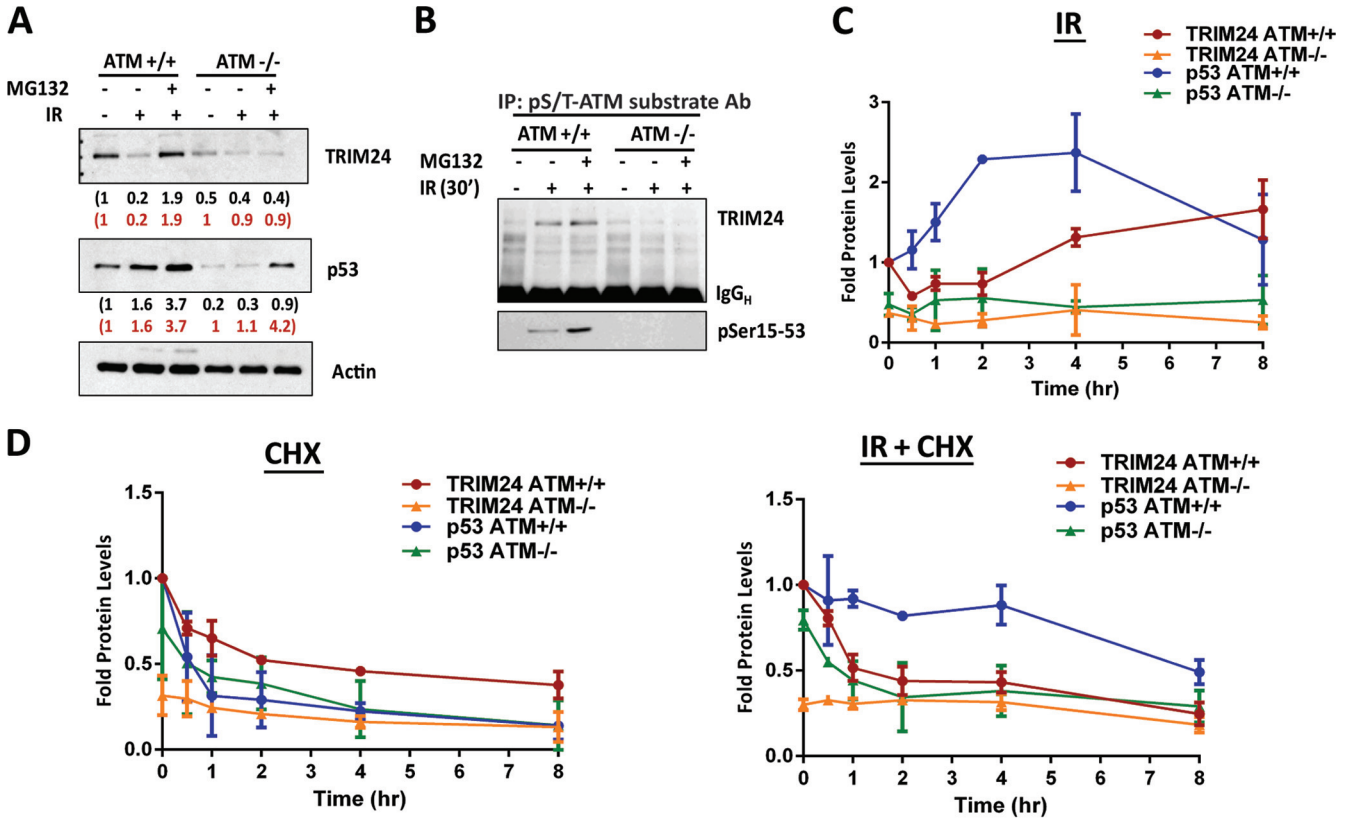

FIG 5 DNA damage-induced degradation of TRIM24 is dependent on ATM. (A) Wild-type ($ATM^{+/+}$) and ATM-null ($ATM^{-/-}$) fibroblasts were collected 1 h after IR exposure with or without MG132 treatment. p53 and TRIM24 protein levels were analyzed by Western blotting and quantified by densitometry. (B) TRIM24 phosphorylation. Wild-type and ATM-null fibroblasts were exposed to IR in the absence or presence of MG132. Total lysates were immunoprecipitated by anti-pS/T ATM substrate antibody and blotted to detect phosphorylated TRIM24 and pSer15-p53. (C and D) TRIM24 protein levels. Wild-type ($ATM^{+/+}$) and ATM-null ($ATM^{-/-}$) fibroblasts were exposed to IR alone, CHX alone, or IR followed by CHX (IR+CHX) and harvested at different time points. TRIM24 and p53 protein were analyzed by Western blotting. The blots were quantified by densitometry, and the average values ± standard errors of the means (error bars) from two experiments are plotted against time.

Ubiquitination of the S768A mutant was also significantly lower than that of wild-type TRIM24 (Fig. 4F), suggesting that ATM-mediated phosphorylation at S768 renders TRIM24 more prone to ubiquitin-mediated degradation. We mutated residue S768 to encode aspartic acid, as a mimetic of phosphorylation, at this site of TRIM24 (S768D) and analyzed its interactions with p53 (see Fig. S3F). Cointeraction analysis in MCF7 cells, transfected with mutant Flag-TRIM24, revealed that the phosphomutant (S768A) rather than the phosphomimic (S768D) interacts more strongly with p53 (see Fig. S3E). In addition, in comparison to wild-type TRIM24, the S768D mutant is less stable (half-life [$t_{1/2}$] of ~2 h) and unchanged by adriamycin treatment (Fig. 4G and Fig. S3G). These results suggest that phosphorylation destabilizes TRIM24 and reduces its association with p53.

In order to confirm that phosphorylation and degradation are initiated by ATM-induced phosphorylation of TRIM24, we analyzed TRIM24 status in wild-type ($ATM^{+/+}$) and ATM-null ($ATM^{-/-}$) human fibroblasts exposed to DNA damage. In healthy wild-type fibroblasts, TRIM24 protein degraded rapidly after IR exposure (20% remaining), which was rescued in the presence of MG132 (Fig. 5A). Interestingly, $ATM^{-/-}$ cells had very low levels of endogenous TRIM24, which were unaffected by either IR or MG132 (Fig. 5A). p53 was activated by IR (~1.6-fold) and by IR and MG132 combined (~3.7-fold) in wild-type cells, but no significant effect of IR alone was seen in cells lacking ATM, although MG132 stabilized p53 in these cells (Fig. 5A). ATM-mediated phosphorylation analysis showed that endogenous TRIM24 and p53 were phosphorylated in response to IR in wild-type cells but not in $ATM^{-/-}$ cells (Fig. 5B). In response to IR, TRIM24 was rapidly degraded (50% within 30 min), whereas p53 stability increased more than 2-fold. This was followed by an increase in TRIM24 levels, while p53 levels returned to the normal threshold at 8 h posttreatment, when the damage response waned (Fig. 5C; see Fig. S4A in the supplemental material). Interestingly, there was no significant effect on TRIM24 degradation or p53 stability after DNA damage in ATM-null cells (Fig. 5C; see Fig. S4A). Similarly, gene expression analysis in MCF7 cells revealed that expression of p53-downstream targets *CDKN1A*, *MDM2*, and *Puma* peaked at 4 h post-IR and 8 h of adriamycin treatments, followed by downregulation, which suggests that p53 transcriptional activity parallels protein levels of p53 after DNA damage response (see Fig. S4B and C).

ATM depletion did not significantly affect the half-lives of either TRIM24 or p53 under homeostatic conditions (Fig. 5D, CHX [cycloheximide]). However, in response to DNA damage (IR plus CHX), TRIM24 degraded rapidly in $ATM^{+/+}$ cells coincident with an elongated p53 half-life (Fig. 5D; see Fig. S4D in the supplemental material). Together, these observations suggest that

ATM kinase acts at the core of the p53-TRIM24 axis: ATM-mediated phosphorylation is sufficient to induce TRIM24 degradation in response to DNA damage, while p53 is stabilized. ATM phosphorylates and activates p53, as well as phosphorylates and destabilizes TRIM24, to yield a synergistic effect on p53 activation.

p53 activates *TRIM24* transcription after DNA damage. We observed that treatment of MCF7 cells and human fibroblasts with DNA-damaging agents led to TRIM24 accumulation after the DNA damage response subsided (Fig. 2C and 5C), which suggests a stress-dependent regulation of TRIM24 levels. Stress-dependent transcriptional activation of E3-ubiquitin ligases that target p53 has been reported previously (44, 45), so we assessed whether TRIM24 was regulated in a similar fashion. Treatment with adriamycin for 24 h resulted in an ~2-fold increase in TRIM24 protein levels in MCF7 and U2OS cells (Fig. 6A; see Fig. S5A in the supplemental material). In parallel, the MDM2 protein level peaked at 12 h after adriamycin treatment and subsided to normal levels at 24 h, at which point TRIM24 levels were at their maximum (Fig. 6A). This suggests a dynamic control of p53 negative regulators that, in turn, play specific roles in achieving tight control over p53 levels.

TRIM24 induction after adriamycin treatment did not occur in the presence of cycloheximide, suggesting that TRIM24 is synthesized *de novo* in response to DNA damage (Fig. 6B). Further, adriamycin treatment resulted in significant induction of *TRIM24* mRNA, similar to induction of p53-downstream targets *CDKN1A* (p21) and *MDM2*, suggesting that TRIM24 transcription is also induced after DNA damage (Fig. 6C). Interestingly, siRNA-mediated depletion of p53 resulted in the complete abrogation of induction of *TRIM24*, *MDM2*, and *CDKN1A* (Fig. 6C). We generated MCF7 cells stably depleted of p53 using short hairpin RNA (shTP53) to determine the effects of p53 on TRIM24 induction in response to DNA damage (Fig. 6D and E; see Fig. S5B to D in the supplemental material). Among three different shRNAs that target *TP53*, shRNA-2 and shRNA-3 resulted in significant (~80%) knockdown of p53 RNA and protein (see Fig. S5B). Interestingly, depletion of p53 also resulted in a significant decrease in TRIM24 protein and RNA levels (see Fig. S5B). Low doses of adriamycin (100 and 250 ng/ml) resulted in significant induction of TRIM24 RNA and protein (up to an 8-fold and 2-fold increase, respectively), similar to *CDKN1A* and *MDM2*, which was abolished in cells depleted of p53 (Fig. 6D and E, *shTP53 #2* and *#3*). On the other hand, a higher dose of adriamycin (500 ng/ml) did not result in a significant induction of TRIM24 levels (Fig. 6D and E). Similarly, lower endogenous levels of TRIM24 and no DNA damage induction of TRIM24 were observed in p53-null ($p53^{-/-}$) mouse embryonic stem (mES) cells compared to wild-type mES cells (see Fig. S5E). Transient exogenous expression of p53 resulted in TRIM24 induction, whereas expression of MDM2 resulted in a dose-dependent decrease in p53 and TRIM24, indicating that TRIM24 levels are directly correlated with p53 abundance (see Fig. S5F and G). To further determine p53-mediated induction of Trim24, we used immortalized MEFs that express a temperature-regulated form of p53 (Val5 MEFs) (45). A temperature shift from 37°C to 32°C promoted translocation of p53R135V from the cytoplasm to the nuclei of Val5 MEFs and increased Trim24 protein levels within 3 h (Fig. 6F). Induction of Trim24 protein levels upon temperature shift was abrogated in the presence of cycloheximide, suggesting p53-responsive enrichment of Trim24 levels due to new protein synthesis (Fig. 6F). Together, these results suggest that DNA damage induces transcription of *TRIM24* in a p53-dependent manner.

***TRIM24* is a direct gene target of p53.** p53-dependent *TRIM24* induction can be the result of either direct or indirect effects of p53 activation during the DNA damage response. p53 is known to regulate the expression of several genes, including some of its own negative regulators, by directly binding to conserved elements within gene regulatory regions (4). We performed chromatin immunoprecipitation followed by deep sequencing (ChIP-Seq) analysis in mouse and human ES cells treated with adriamycin to determine downstream targets of p53 (46). Apart from previously validated p53 targets, several novel genes likely regulated by p53 were identified. Interestingly, we observed a strong peak of p53 binding on both mouse *Trim24* and human *TRIM24*, which consisted of p53 response elements (p53REs) in intron 1 and upstream of the proximal promoter (approximately −26 kb from the transcription start site), respectively (see Fig. S6A and B in the supplemental material). p53 enrichment at these sites was confirmed by ChIP followed by quantitative PCR (qPCR), using primers flanking p53REs on *TRIM24*, *MDM2*, *CDKN1A*, and *Trim24* (see Fig. S6B for locations of p53REs). Adriamycin treatment resulted in enrichment of p53 at p53REs on both mouse and human *TRIM24* (Fig. 7A and B), suggesting that p53-mediated activation of TRIM24 is conserved across species. p53 enrichment on TRIM24 is comparable to levels of p53 binding to p53REs on *CDKN1A* and *MDM2* in both mouse and human cells (Fig. 7A and B). Furthermore, a significant enrichment of p53 on *TRIM24* was also observed in human and mouse ES cells treated with adriamycin (see Fig. S6C). Taken together, these results suggest that, in response to DNA damage, p53 activates TRIM24 transcription by directly binding to p53REs; thus, we have identified *TRIM24* as a previously unknown target of p53.

TRIM24 preferentially targets phosphorylated p53. A striking aspect of p53 signaling, in response to stress or inductive signaling, is the tightly regulated process of posttranscriptional modifications (PTMs) of p53 that determines the physiological outcomes of p53 activation. PTMs of p53 occur on more than 40 different amino acid residues and likely provide fine-tuning and specificity for p53 activation (5, 7). Cointeraction analysis in MCF7 cells, transfected with Flag-TRIM24 and treated with adriamycin for various lengths of time or exposed to IR and collected at different time points, revealed a significant interaction between p53 and TRIM24 at relatively late times after DNA damage (at 24 h of adriamycin treatment and at 2 h after IR exposure) (Fig. 8A and B). Although this could be simply a reflection of increased levels of total p53, since TRIM24 levels were normalized, detection of damage-induced pSer15-p53 in inputs after IR treatment showed that pSer15-p53 levels did not increase when p53 levels rose over 2 h (Fig. 8B). The interaction between TRIM24 and p53 was significantly abrogated when the cell lysates were treated with calf intestinal phosphatase (CIP) *in vitro* to remove phosphorylation of p53, as shown by the absence of pSer15-p53 (compare the two 2h lanes in Fig. 8B). In order to expand on these observations, we immunoprecipitated lysates from MCF7 cells exposed to adriamycin for different time points with a pSer15-p53 antibody and observed a significant enrichment of TRIM24 at 8 and 24 h after adriamycin treatment (Fig. 8C). We treated MCF7 cells with nutlin 3, a selective small-molecule antagonist of MDM2 (47) and observed a dramatic stabilization of p53 protein that is not phosphorylated at Ser15 (Fig. 8D). Coimmunoprecipitation analysis

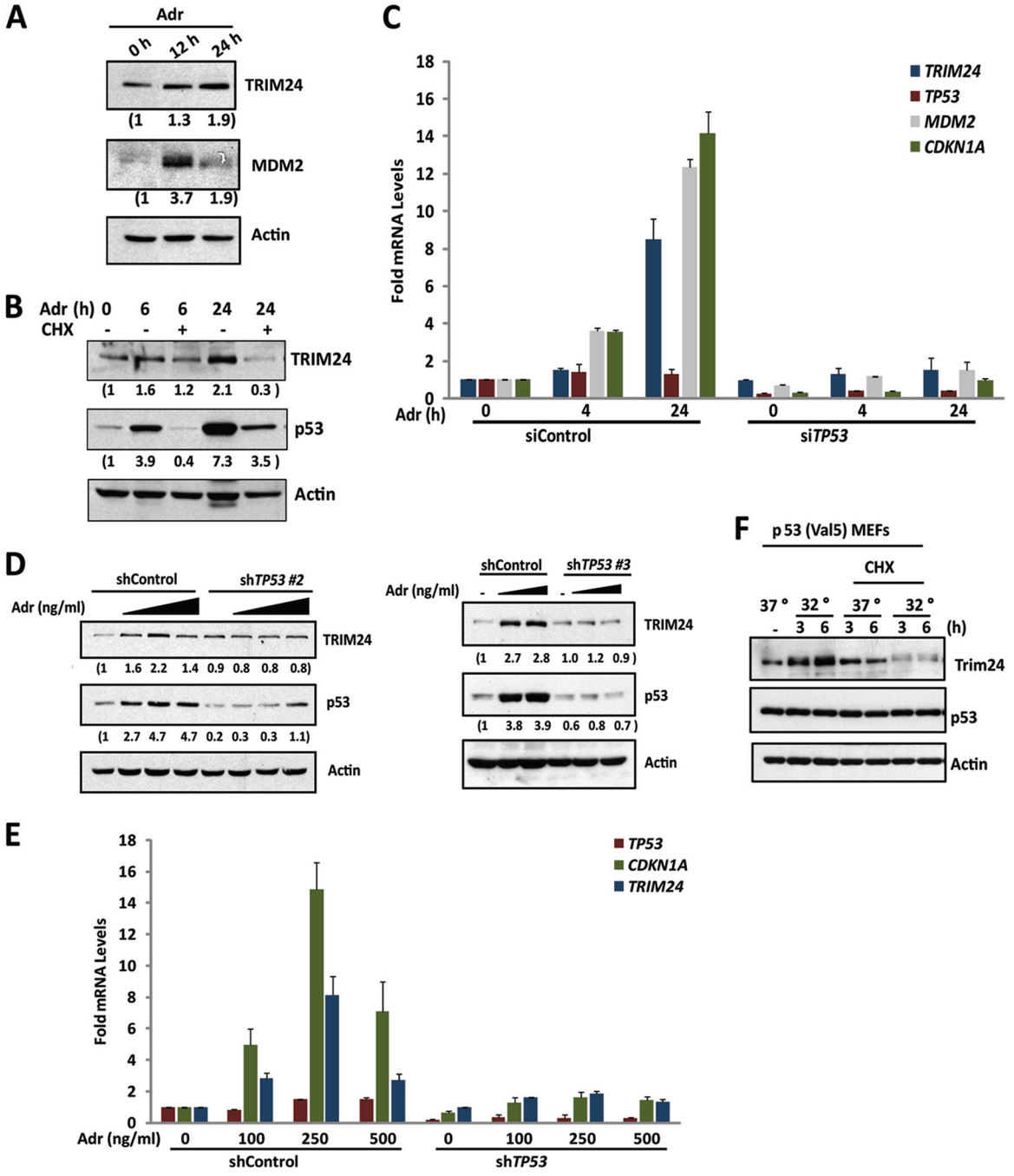

FIG 6 p53 activates *TRIM24* transcription after DNA damage. (A) Total lysates from MCF7 cells treated with Adr (250 ng/ml) for different lengths of time were immunoblotted to detect TRIM24, MDM2, and p53 protein levels. (B) Total lysates from MCF7 cells treated with Adr for the indicated lengths of time in the absence or presence of CHX were immunoblotted to detect TRIM24 and p53. (C) Quantitative real-time PCR (qRT-PCR) assay. MCF7 cells were transfected with nontarget siRNA (siControl) or siRNA specific to p53 (si*TP53*) and treated with Adr for different lengths of time. RNA prepared from these cells was subjected to qRT-PCR assay with primers specific for *TP53*, *TRIM24*, *MDM2*, and *CDKN1A*. (D and E) MCF7 cells stably expressing nontarget shRNA (shControl) or shRNAs specific to p53 (sh*TP53*) (clones 2 and 3) were treated with different doses (0, 100, 250, and 500 ng/ml) of adriamycin for 24 h. Protein levels were analyzed by Western blotting (D), and RNA levels were analyzed by qRT-PCR (E). (F) Trim24 protein levels in Val5 cells 3 and 6 h after a shift to 32°C in the presence of absence of CHX.

revealed that TRIM24 preferentially bound to modified p53 as a result of adriamycin treatment but not to the unmodified stable p53 resulting from nutlin 3 treatment (Fig. 8D). We determined pSer15-p53 levels with adriamycin treatment over time and observed that clearance of pSer15-p53 upon removal of adriamycin was significantly slower in cells depleted of TRIM24 than in control cells, which suggests TRIM24-dependent degradation of phosphorylated p53 (see Fig. S7A in the supplemental material). Similarly, in response to adriamycin treatment, the kinetics of pSer15-p53 clearance was much slower in mouse ES cells stably

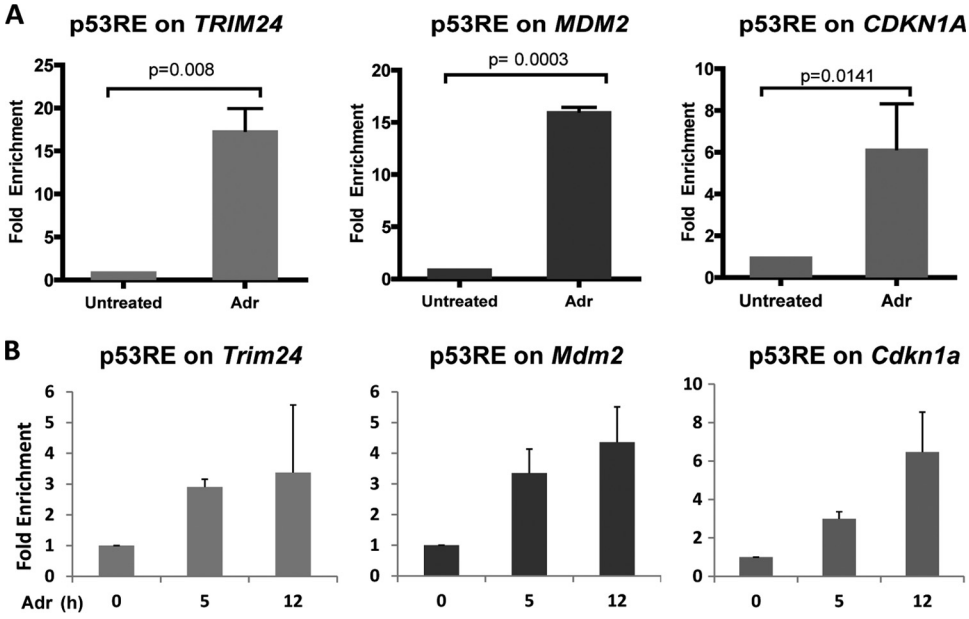

FIG 7 TRIM24 is a direct gene target of p53. (A) p53 ChIP analysis in human cells. p53-bound chromatin was immunoprecipitated from MCF7 cells treated with Adr for 12 h, and p53 enrichment on *TRIM24*, *MDM2*, and *CDKN1A* was analyzed by qPCR using primers encompassing p53REs and plotted as the fold increase in p53 enrichment compared to input. (B) p53 ChIP analysis in mouse ES cells. p53-bound chromatin was immunoprecipitated from mES cells treated with Adr for 5 or 12 h, and p53 enrichment on *Trim24*, *Mdm2*, and *Cdkn1a* was analyzed by qPCR using primers encompassing p53REs and plotted as the fold increase in p53 enrichment compared to input.

depleted of Trim24 (see Fig. S7B). Taken together, these results suggest that TRIM24 preferentially binds to and targets phosphorylated p53 for degradation. We propose that this interaction and subsequent degradation of p53 act in terminating p53 activity and prevent prolonged induction of p53 functions during cellular recovery from DNA damage.

DISCUSSION

Here, we describe an autoregulatory feedback loop between p53 and E3-ubiquitin ligase TRIM24 during the DNA damage response (Fig. 8D). TRIM24 was recently identified as a p53-interacting partner and E3-ubiquitin ligase of p53 in both embryonic stem cells and breast cancer cells (19). Additionally, TRIM24 is a coactivator of ER-α and binds estrogen response elements of ER-regulated genes implicated in cellular proliferation and neoplasia of breast cancer cells (23, 48, 49). The mechanisms that regulate TRIM24 in breast cancers, where TRIM24 is frequently and aberrantly overexpressed, remain largely unknown, although deregulation of E3-ubiquitin ligases is a common theme in human cancers (50).

Our current studies show that levels of endogenous TRIM24 decrease in response to DNA damage by a mechanism similar to DNA damage-mediated regulation of other p53 E3-ubiquitin ligases: MDM2, MDM4, and COP1 (29, 33, 34). DNA damage induces ATM kinase, which directly phosphorylates p53 at Ser15 (38) and Ser768 of TRIM24 (shown here). The presence of TRIM24 phosphorylated at Ser768 after DNA damage is early and transient: forewarning of MDM2-independent degradation and decline of TRIM24. On the basis of the timing and TRIM24 dependence of these events, we suggest that ATM kinase mediates a conformational change in TRIM24 structure that directs its ubiquitination activity to itself. This leads to TRIM24 degradation early in response to DNA damage, facilitating robust p53 activation and initiation of a DNA repair program.

After sufficient DNA repair has occurred, high levels of p53 must be reduced to the normal low levels below a threshold that induces stress response in cells. A prolonged activation of p53 is likely detrimental to full recovery of cells and return to cellular homeostasis. p53-induced autoregulatory feedback loops, as well characterized for MDM2 (11–13), maintain the normal low levels of p53 due to downstream activation of p53 negative regulators, as direct gene targets of activated p53. Accordingly, TRIM24 transcription is activated by direct binding of activated p53 to conserved p53REs, newly identified here within intron 1 of mouse *Trim24* and upstream of the transcription start site of human *TRIM24*. Thus, DNA damage-mediated activation of TRIM24 is directly dependent on p53's transcriptional activity, similar to mechanisms of control reported for other negative regulators of p53: MDM2, COP1, and Pirh2 (44, 51, 52). Translation of increased *TRIM24* mRNA promotes the accumulation of *de novo*-synthesized TRIM24, which is not phosphorylated at Ser768 in the absence of additional stress. This population of TRIM24 then targets phosphorylated p53 for degradation and a return to the normal low levels of p53.

The mechanisms of p53 activation have been studied in considerable detail, although significantly less is known about termination of the p53 response to stress signaling (53). Since p53 controls the expression of genes involved in a number of critical pathways in addition to tumor suppression and DNA repair, tight control over its availability for transcription regulation is required (4). One of the major mechanisms that limits the existence of p53 protein is ubiquitin-mediated degradation. Covalent tagging of p53 with polyubiquitin chains targets the protein for proteasomal degradation in healthy cells. MDM2 was the first identified E3-

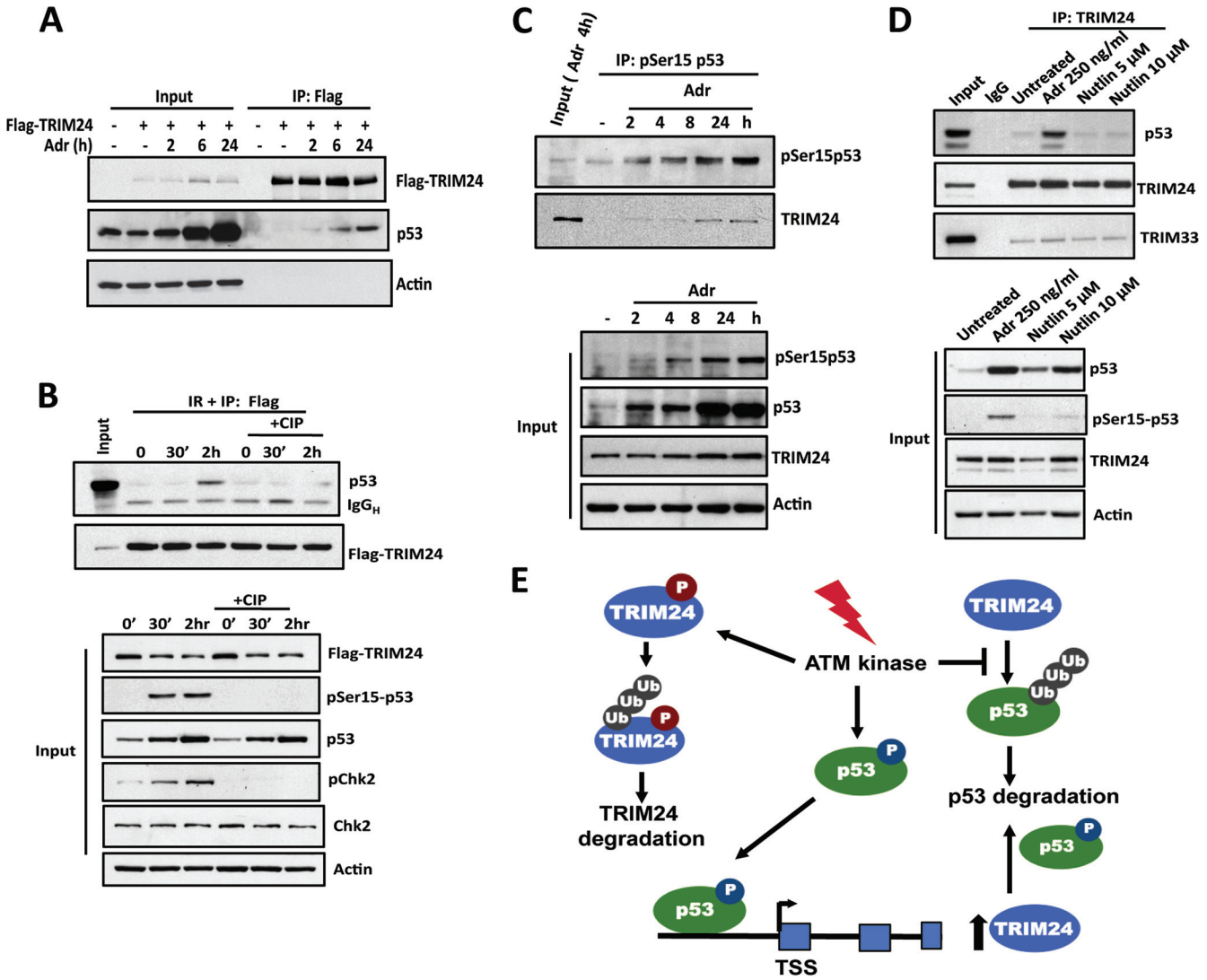

FIG 8 TRIM24 preferentially targets phosphorylated p53. (A to D) TRIM24-p53 interaction. (A) MCF7 cells were transfected with Flag-TRIM24 plasmids, followed by treatment with Adr for different lengths of time. Total cell lysates were immunoprecipitated with Flag antibody and immunoblotted for Flag, p53, and actin. (B) MCF7 cells transfected with Flag-TRIM24 plasmid were exposed to IR. The cell lysates were incubated with calf intestinal phosphatase (CIP) for 1 h and subjected to immunoprecipitation with Flag antibody, followed by immunoblotting with Flag and p53. Inputs were also probed with pSer15-p53 and pCHK2 to confirm dephosphorylation (bottom blots). (C) Lysates from MCF7 cells treated with Adr for different lengths of time were immunoprecipitated with pSer15-p53 antibody and immunoblotted with TRIM24 and pSer15-p53. Inputs are shown in the bottom blots. (D) Lysates from MCF7 cells treated with Adr or nutlin for 24 h were immunoprecipitated with TRIM24 antibody and immunoblotted with TRIM24, p53, and TRIM33. Inputs were also probed with pSer15-p53 to determine p53 phosphorylation (bottom blots). (E) Model demonstrating the autoregulatory feedback loop between p53 and TRIM24. TRIM24 targets endogenous p53 for ubiquitin-mediated degradation. DNA damage activates ATM kinase that phosphorylates p53, resulting in its stabilization and activation. Active p53 then induces transcription of downstream genes, including TRIM24. In parallel, ATM kinase phosphorylates S768 of TRIM24, which dissociates TRIM24 from p53 and targets itself for autodestruction via its RING domain. Further, active p53 directly binds to p53RE on *TRIM24*, resulting in *TRIM24* transcription activation in response to DNA damage. During the postdamage recovery phase, newly synthesized TRIM24 preferentially interacts with phosphorylated p53 and targets it for degradation in order to bring excess p53 back to normal threshold levels, thus completing a negative-feedback loop. P, phosphate group; TSS, transcription start site.

ubiquitin ligase responsible for the degradation of p53 (11–13). Subsequently, several other ubiquitin ligases such as Pirh2, COP1, and ARF-BP1 were identified with either RING-E3 or HECT-E3 activity that act independently of MDM2. These E3-ubiquitin ligases negatively regulate p53 by either controlling endogenous basal levels or degrading activated p53 (16, 17, 44, 52, 54). Thus, cells possess intricate machinery consisting of several proteins and regulatory pathways that converge on p53.

Our results highlight a previously unknown mechanism in regulation of the p53 pathway, which occurs via modulation of a TRIM24-p53 axis during DNA damage. Although TRIM24 is not the sole E3-ubiquitin ligase capable of shutting down p53 response, its increased expression in breast cancer cells that express wild-type p53, as well as high expression and negative correlation with survival of breast cancer patients (23), suggest that E3-ubiquitin ligases may exhibit a tissue- or context-specific hierarchy in targeting p53 for degradation. TRIM24 lies at the intersection of signaling pathways regulated by p53 and/or nuclear receptors, in-

creasing the complexity of tissue-specific interpretation of function. Further analysis of the *in vivo* functions of TRIM24, as well as other E3-ubiquitin ligases of p53, is required to determine the tissue or stress specificity of these regulators and their downstream effects on genome stability and cellular homeostasis.

ACKNOWLEDGMENTS

This work was supported by funds from Cancer Prevention and Research Initiative of Texas grant RP100602 to M.C.B. and the NCI Cancer Center Support Grant to the University of Texas M. D. Anderson Cancer Center. A.K.J. was supported in part by the Laura and John Arnold Foundation and the Odyssey Scholars Program at the University of Texas M. D. Anderson Cancer Center.

We are grateful to the members of our laboratory for help with this work.

REFERENCES

1. **Vousden KH, Lane DP.** 2007. p53 in health and disease. Nat. Rev. Mol. Cell Biol. **8:**275–283. http://dx.doi.org/10.1038/nrm2147.
2. **Vogelstein B, Lane D, Levine AJ.** 2000. Surfing the p53 network. Nature **408:**307–310. http://dx.doi.org/10.1038/35042675.
3. **Lavin MF, Gueven N.** 2006. The complexity of p53 stabilization and activation. Cell Death Differ. **13:**941–950. http://dx.doi.org/10.1038/sj.cdd.4401925.
4. **Vousden KH, Prives C.** 2009. Blinded by the light: the growing complexity of p53. Cell **137:**413–431. http://dx.doi.org/10.1016/j.cell.2009.04.037.
5. **Bode AM, Dong Z.** 2004. Post-translational modification of p53 in tumorigenesis. Nat. Rev. Cancer **4:**793–805. http://dx.doi.org/10.1038/nrc1455.
6. **Toledo F, Wahl GM.** 2006. Regulating the p53 pathway: in vitro hypotheses, in vivo veritas. Nat. Rev. Cancer **6:**909–923. http://dx.doi.org/10.1038/nrc2012.
7. **Murray-Zmijewski F, Slee EA, Lu X.** 2008. A complex barcode underlies the heterogeneous response of p53 to stress. Nat. Rev. Mol. Cell Biol. **9:**702–712. http://dx.doi.org/10.1038/nrm2451.
8. **Carter S, Vousden KH.** 2009. Modifications of p53: competing for the lysines. Curr. Opin. Genet. Dev. **19:**18–24. http://dx.doi.org/10.1016/j.gde.2008.11.010.
9. **Kruse JP, Gu W.** 2009. Modes of p53 regulation. Cell **137:**609–622. http://dx.doi.org/10.1016/j.cell.2009.04.050.
10. **Montes de Oca Luna R, Wagner DS, Lozano G.** 1995. Rescue of early embryonic lethality in mdm2-deficient mice by deletion of p53. Nature **378:**203–206. http://dx.doi.org/10.1038/378203a0.
11. **Haupt Y, Maya R, Kazaz A, Oren M.** 1997. Mdm2 promotes the rapid degradation of p53. Nature **387:**296–299. http://dx.doi.org/10.1038/387296a0.
12. **Honda R, Tanaka H, Yasuda H.** 1997. Oncoprotein MDM2 is a ubiquitin ligase E3 for tumor suppressor p53. FEBS Lett. **420:**25–27. http://dx.doi.org/10.1016/S0014-5793(97)01480-4.
13. **Kubbutat MH, Jones SN, Vousden KH.** 1997. Regulation of p53 stability by Mdm2. Nature **387:**299–303. http://dx.doi.org/10.1038/387299a0.
14. **Ringshausen I, O'Shea CC, Finch AJ, Swigart LB, Evan GI.** 2006. Mdm2 is critically and continuously required to suppress lethal p53 activity in vivo. Cancer Cell **10:**501–514. http://dx.doi.org/10.1016/j.ccr.2006.10.010.
15. **Pant V, Xiong S, Jackson JG, Post SM, Abbas HA, Quintas-Cardama A, Hamir AN, Lozano G.** 2013. The p53-Mdm2 feedback loop protects against DNA damage by inhibiting p53 activity but is dispensable for p53 stability, development, and longevity. Genes Dev. **27:**1857–1867. http://dx.doi.org/10.1101/gad.227249.113.
16. **Jain AK, Barton MC.** 2009. Regulation of p53: TRIM24 enters the RING. Cell Cycle **8:**3668–3674. http://dx.doi.org/10.4161/cc.8.22.9979.
17. **Jain AK, Barton MC.** 2010. Making sense of ubiquitin ligases that regulate p53. Cancer Biol. Ther. **10:**665–672. http://dx.doi.org/10.4161/cbt.10.7.13445.
18. **Brooks CL, Gu W.** 2006. p53 ubiquitination: Mdm2 and beyond. Mol. Cell **21:**307–315. http://dx.doi.org/10.1016/j.molcel.2006.01.020.
19. **Allton K, Jain AK, Herz HM, Tsai WW, Jung SY, Qin J, Bergmann A, Johnson RL, Barton MC.** 2009. Trim24 targets endogenous p53 for degradation. Proc. Natl. Acad. Sci. U. S. A. **106:**11612–11616. http://dx.doi.org/10.1073/pnas.0813177106.
20. **Reymond A, Meroni G, Fantozzi A, Merla G, Cairo S, Luzi L, Riganelli D, Zanaria E, Messali S, Cainarca S, Guffanti A, Minucci S, Pelicci PG, Ballabio A.** 2001. The tripartite motif family identifies cell compartments. EMBO J. **20:**2140–2151. http://dx.doi.org/10.1093/emboj/20.9.2140.
21. **Meroni G, Diez-Roux G.** 2005. TRIM/RBCC, a novel class of 'single protein RING finger' E3 ubiquitin ligases. Bioessays **27:**1147–1157. http://dx.doi.org/10.1002/bies.20304.
22. **Le Douarin B, Nielsen AL, Garnier JM, Ichinose H, Jeanmougin F, Losson R, Chambon P.** 1996. A possible involvement of TIF1 alpha and TIF1 beta in the epigenetic control of transcription by nuclear receptors. EMBO J. **15:**6701–6715.
23. **Tsai WW, Wang Z, Yiu TT, Akdemir KC, Xia W, Winter S, Tsai CY, Shi X, Schwarzer D, Plunkett W, Aronow B, Gozani O, Fischle W, Hung MC, Patel DJ, Barton MC.** 2010. TRIM24 links a non-canonical histone signature to breast cancer. Nature **468:**927–932. http://dx.doi.org/10.1038/nature09542.
24. **Khetchoumian K, Teletin M, Tisserand J, Mark M, Herquel B, Ignat M, Zucman-Rossi J, Cammas F, Lerouge T, Thibault C, Metzger D, Chambon P, Losson R.** 2007. Loss of Trim24 (Tif1alpha) gene function confers oncogenic activity to retinoic acid receptor alpha. Nat. Genet. **39:**1500–1506. http://dx.doi.org/10.1038/ng.2007.15.
25. **Tsai WW, Nguyen TT, Shi Y, Barton MC.** 2008. p53-targeted LSD1 functions in repression of chromatin structure and transcription in vivo. Mol. Cell. Biol. **28:**5139–5146. http://dx.doi.org/10.1128/MCB.00287-08.
26. **Bres V, Kiernan RE, Linares LK, Chable-Bessia C, Plechakova O, Treand C, Emiliani S, Peloponese JM, Jeang KT, Coux O, Scheffner M, Benkirane M.** 2003. A non-proteolytic role for ubiquitin in Tat-mediated transactivation of the HIV-1 promoter. Nat. Cell Biol. **5:**754–761. http://dx.doi.org/10.1038/ncb1023.
27. **Jain AK, Allton K, Iacovino M, Mahen E, Milczarek RJ, Zwaka TP, Kyba M, Barton MC.** 2012. p53 regulates cell cycle and microRNAs to promote differentiation of human embryonic stem cells. PLoS Biol. **10:**e1001268. http://dx.doi.org/10.1371/journal.pbio.1001268.
28. **Wang C, Ivanov A, Chen L, Fredericks WJ, Seto E, Rauscher FJ, III, Chen J.** 2005. MDM2 interaction with nuclear corepressor KAP1 contributes to p53 inactivation. EMBO J. **24:**3279–3290. http://dx.doi.org/10.1038/sj.emboj.7600791.
29. **Stommel JM, Wahl GM.** 2004. Accelerated MDM2 auto-degradation induced by DNA-damage kinases is required for p53 activation. EMBO J. **23:**1547–1556. http://dx.doi.org/10.1038/sj.emboj.7600145.
30. **Marine JC.** 2010. p53 stabilization: the importance of nuclear import. Cell Death Differ. **17:**191–192. http://dx.doi.org/10.1038/cdd.2009.183.
31. **Ogretmen B, Safa AR.** 1997. Expression of the mutated p53 tumor suppressor protein and its molecular and biochemical characterization in multidrug resistant MCF-7/Adr human breast cancer cells. Oncogene **14:**499–506. http://dx.doi.org/10.1038/sj.onc.1200855.
32. **Khosravi R, Maya R, Gottlieb T, Oren M, Shiloh Y, Shkedy D.** 1999. Rapid ATM-dependent phosphorylation of MDM2 precedes p53 accumulation in response to DNA damage. Proc. Natl. Acad. Sci. U. S. A. **96:**14973–14977. http://dx.doi.org/10.1073/pnas.96.26.14973.
33. **Pereg Y, Shkedy D, de Graaf P, Meulmeester E, Edelson-Averbukh M, Salek M, Biton S, Teunisse AF, Lehmann WD, Jochemsen AG, Shiloh Y.** 2005. Phosphorylation of Hdmx mediates its Hdm2- and ATM-dependent degradation in response to DNA damage. Proc. Natl. Acad. Sci. U. S. A. **102:**5056–5061. http://dx.doi.org/10.1073/pnas.0408595102.
34. **Dornan D, Shimizu H, Mah A, Dudhela T, Eby M, O'Rourke K, Seshagiri S, Dixit VM.** 2006. ATM engages autodegradation of the E3 ubiquitin ligase COP1 after DNA damage. Science **313:**1122–1126. http://dx.doi.org/10.1126/science.1127335.
35. **Shiloh Y.** 2003. ATM and related protein kinases: safeguarding genome integrity. Nat. Rev. Cancer. **3:**155–168. http://dx.doi.org/10.1038/nrc1011.
36. **Kastan MB, Onyekwere O, Sidransky D, Vogelstein B, Craig RW.** 1991. Participation of p53 protein in the cellular response to DNA damage. Cancer Res. **51:**6304–6311.
37. **Kastan MB, Radin AI, Kuerbitz SJ, Onyekwere O, Wolkow CA, Civin CI, Stone KD, Woo T, Ravindranath Y, Craig RW.** 1991. Levels of p53 protein increase with maturation in human hematopoietic cells. Cancer Res. **51:**4279–4286.
38. **Banin S, Moyal L, Shieh S, Taya Y, Anderson CW, Chessa L, Smorodinsky NI, Prives C, Reiss Y, Shiloh Y, Ziv Y.** 1998. Enhanced phosphorylation of p53 by ATM in response to DNA damage. Science **281:**1674–1677. http://dx.doi.org/10.1126/science.281.5383.1674.

39. **Dumaz N, Meek DW.** 1999. Serine15 phosphorylation stimulates p53 transactivation but does not directly influence interaction with HDM2. EMBO J. **18:**7002–7010. http://dx.doi.org/10.1093/emboj/18.24.7002.
40. **Maya R, Balass M, Kim ST, Shkedy D, Leal JF, Shifman O, Moas M, Buschmann T, Ronai Z, Shiloh Y, Kastan MB, Katzir E, Oren M.** 2001. ATM-dependent phosphorylation of Mdm2 on serine 395: role in p53 activation by DNA damage. Genes Dev. **15:**1067–1077. http://dx.doi.org/10.1101/gad.886901.
41. **Bakkenist CJ, Kastan MB.** 2003. DNA damage activates ATM through intermolecular autophosphorylation and dimer dissociation. Nature **421:**499–506. http://dx.doi.org/10.1038/nature01368.
42. **Matsuoka S, Ballif BA, Smogorzewska A, McDonald ER, III, Hurov KE, Luo J, Bakalarski CE, Zhao Z, Solimini N, Lerenthal Y, Shiloh Y, Gygi SP, Elledge SJ.** 2007. ATM and ATR substrate analysis reveals extensive protein networks responsive to DNA damage. Science **316:**1160–1166. http://dx.doi.org/10.1126/science.1140321.
43. **Kurz EU, Douglas P, Lees-Miller SP.** 2004. Doxorubicin activates ATM-dependent phosphorylation of multiple downstream targets in part through the generation of reactive oxygen species. J. Biol. Chem. **279:**53272–53281. http://dx.doi.org/10.1074/jbc.M406879200.
44. **Leng RP, Lin Y, Ma W, Wu H, Lemmers B, Chung S, Parant JM, Lozano G, Hakem R, Benchimol S.** 2003. Pirh2, a p53-induced ubiquitin-protein ligase, promotes p53 degradation. Cell **112:**779–791. http://dx.doi.org/10.1016/S0092-8674(03)00193-4.
45. **Wu X, Bayle JH, Olson D, Levine AJ.** 1993. The p53-mdm-2 autoregulatory feedback loop. Genes Dev. **7:**1126–1132. http://dx.doi.org/10.1101/gad.7.7a.1126.
46. **Akdemir KC, Jain AK, Allton K, Aronow B, Xu X, Cooney AJ, Li W, Barton MC.** 2014. Genome-wide profiling reveals stimulus-specific functions of p53 during differentiation and DNA damage of human embryonic stem cells. Nucleic Acids Res. **42:**205–223. http://dx.doi.org/10.1093/nar/gkt866.
47. **Vassilev LT, Vu BT, Graves B, Carvajal D, Podlaski F, Filipovic Z, Kong N, Kammlott U, Lukacs C, Klein C, Fotouhi N, Liu EA.** 2004. In vivo activation of the p53 pathway by small-molecule antagonists of MDM2. Science **303:**844–848. http://dx.doi.org/10.1126/science.1092472.
48. **Katzenellenbogen BS.** 1996. Estrogen receptors: bioactivities and interactions with cell signaling pathways. Biol. Reprod. **54:**287–293. http://dx.doi.org/10.1095/biolreprod54.2.287.
49. **Cheskis BJ, Greger JG, Nagpal S, Freedman LP.** 2007. Signaling by estrogens. J. Cell. Physiol. **213:**610–617. http://dx.doi.org/10.1002/jcp.21253.
50. **Chen C, Seth AK, Aplin AE.** 2006. Genetic and expression aberrations of E3 ubiquitin ligases in human breast cancer. Mol. Cancer Res. **4:**695–707. http://dx.doi.org/10.1158/1541-7786.MCR-06-0182.
51. **Barak Y, Juven T, Haffner R, Oren M.** 1993. mdm2 expression is induced by wild type p53 activity. EMBO J. **12:**461–468.
52. **Dornan D, Wertz I, Shimizu H, Arnott D, Frantz GD, Dowd P, O'Rourke K, Koeppen H, Dixit VM.** 2004. The ubiquitin ligase COP1 is a critical negative regulator of p53. Nature **429:**86–92. http://dx.doi.org/10.1038/nature02514.
53. **Harris SL, Levine AJ.** 2005. The p53 pathway: positive and negative feedback loops. Oncogene **24:**2899–2908. http://dx.doi.org/10.1038/sj.onc.1208615.
54. **Chen D, Kon N, Li M, Zhang W, Qin J, Gu W.** 2005. ARF-BP1/Mule is a critical mediator of the ARF tumor suppressor. Cell **121:**1071–1083. http://dx.doi.org/10.1016/j.cell.2005.03.037.